Inorg. Chem. **2002**, *41*, 1831–1836

Effect of Asymmetry on the Electronic Delocalization in Diiron and Iron–Cobalt Mixed Valence Metallocenic Compounds

Y. Portilla, I. Chávez,* V. Arancibia, B. Loeb, and J. M. Manríquez*

Pontificia Universidad Católica de Chile, Facultad de Química, Casilla 306, Correo 22, Santiago, Chile

A. Roig and E. Molins

Institut de Ciència de Materials de Barcelona (ICMAB-CSIC), Campus UAB, 08193 Bellaterra, Barcelona, España

Received November 16, 2001

In this work, we report the synthesis and a study on the degree of electronic delocalization in the asymmetric mixed valence complexes $[Cp^*Fe(C_8H_6)Fe(C_8H_7)]^+$, **3a**$^+$, and $[Cp^*Co(C_8H_6)Fe(C_8H_7)]^+$, **3b**$^+$, ($Cp^* = C_5Me_5$, C_8H_6 = pentalenyde, C_8H_7 = hydropentalenyde, and $BAr'_4 = ((3,5(CF_3)_2C_6H_3)_4B^-)$). Electrochemical methods, ^{57}Fe Mössbauer spectroscopy, electronic spectroscopy, and electron paramagnetic resonance were used for this purpose. Although the anti conformation of the complexes precludes any metal–metal interaction, all the techniques employed show that **3a**$^+$ is a electronic delocalized system, while **3b**$^+$ behaves as two individual metallic centers with localized electron density.

Introduction

Mixed valence (MV) complexes have been of general interest for a long time.[1] Among them, organometallic systems have received considerable attention.[2] Specifically, over the past decade, there has been remarkable progress in understanding the influence of different parameters on intramolecular electron-transfer rates in mixed valence biferrocenium cations. Factors such as lattice dynamics,[2c−d,3−5] cation−anion interactions,[6−8] structural micromodifications,[9] influence of cyclopentadienil ring tilt,[10,11] effects of asymmetric substitution,[2b,12−14] as well as the symmetry of the cation[15] have been considered.

Most of the studies reported concerning electron transfer in homonuclear asymmetric substituted mixed valence complexes of iron have dealt with biferrocenes substituted either at the fulvalenide ligand or at one or both of the cyclopentadienide ligands. (The term *homonuclear* is used here for compounds with identical metals, and *heteronuclear* for compounds with two different metals. On the other hand,

* To whom correspondence should be addressed. E-mail: jmanriqm@puc.cl.

(1) (a) Robin, M. B.; Day, P. *Adv. Inorg. Chem. Radiochem*. **1967**, *10*, 247. (b) Hush, N. S. *Prog. Inorg. Chem*. **1967**, *8*, 391. (c) *Mixed Valence Compounds*; Brown, D. B., Ed.; D. Reidel Pub. Co.: Dordrecht, Holland, 1980. (d) *Mixed Valency Systems: Applications in Chemistry, Physics and Biology*; Prassides, K., Ed.; Kluwer Academic Publishers: Dordrecht, The Netherlands, 1991.

(2) (a) Cowan, D. O.; Collins, R. L.; Kaufman, F. *J. Phys. Chem*. **1971**, *75*, 2025. (b) Le Vanda, C.; Bechgaard, K.; Cowan, D. O.; Rausch, M. D. *J. Am. Chem. Soc*. **1977**, *99*, 2964. (c) Dong, T.-Y.; Hendrickson, D. N.; Iwai, K.; Cohn, M. J.; Geib, S. J.; Rheingold, A. L.; Sano, H.; Motoyama, I.; Nakashima, S. *J. Am. Chem. Soc*. **1985**, *107*, 7996. (d) Iijima, S.; Saida, R.; Motoyama, I.; Sano, H. *Bull. Chem. Soc. Jpn*. **1981**, *54*, 1375.

(3) Cohn, M. J.; Dong, T.-Y.; Hendrickson, D. N.; Geib, S. J.; Rheingold, A. L. *J. Chem. Soc., Chem. Commun*. **1985**, 1095.

(4) Nakashima, S.; Katada, M.; Motoyama, I.; Sano, H. *Bull. Chem. Soc. Jpn*. **1987**, *54*, 1375.

(5) Kai, M.; Katada, M.; Sano, H. *Chem. Lett*. **1988**, 1523.

(6) Kambara, T.; Hendrickson, D. N.; Dong, T.-Y.; Cohn, M. J. *J. Chem. Phys*. **1987**, *86*, 2362.

(7) Dong, T.-Y.; Huang, C. H.; Chang, C. K.; Hsieh, H. C.; Peng, S. M.; Lee, G. H. *Organometallics* **1995**, *14*, 1776.

(8) Dong, T.-Y.; Schei, C. C.; Hwang, M. Y.; Lee, T. Y.; Yeh, S. K.; Wen, Y. S. *Organometallics* **1992**, *11*, 573.

(9) Dong, T.-Y.; Lee, T. Y.; Lee, S. H.; Lee, G. H.; Peng, S. M. *Organometallics* **1994**, *13*, 2337.

(10) Dong, T.-Y.; Chang, C. K.; Huang, C. H.; Wen, Y. S.; Lee, S. L.; Chen, J. A.; Yeh, W. Y.; Yeh, A. J. *J. Chem. Soc., Chem. Commun*. **1992**, 526.

(11) Dong, T.-Y.; Huang, C. H.; Chang, C. K.; Wen, Y. S.; Lee, S. L.; Chen, J. A.; Yeh, W. Y.; Yeh, A. J. *J. Am. Chem. Soc*. **1993**, *115*, 6357.

(12) Dong, T.-Y.; Lin, P.-J.; Lin, K.-J. *Inorg. Chem*. **1996**, *35*, 6037.

(13) Dong, T.-Y.; Schei, C.-C.; Hsu, T.-L.; Lee, S.-L.; Li, S.-J. *Inorg. Chem*. **1991**, *30*, 2457.

(14) Moore, M. F.; Hendrickson, D. N. *Inorg. Chem*. **1985**, *24*, 1236.

(15) Nakashima, S.; Oda, T.; Okuda, T.; Watanabe, M. *Inorg. Chem*. **1999**, *38*, 4005.

10.1021/ic011175s CCC: $22.00
Published on Web 03/13/2002

the term *asymmetric* will be used to express different ligand environments for the two metals.) These types of compounds have been found to be localized on the ^{57}Fe Mössbauer time scale, at low temperature. In nearly all the cases reported, the corresponding symmetric unsubstituted derivative belongs to class II according to the classification of Robin and Day.[1a] Also, in agreement with Hush's prediction,[1b] a displacement to higher energy of the intervalence transfer (IT) electronic absorption band compared to the IT band for unsubstituted mixed valence biferrocene was observed.

Until now, (3-acetylfulvalene)(fulvalene)diiron monocation, **1b**$^+$, reported by Hendrickson and Moore,[14] appears to be the only example of an asymmetric substituted mixed valence diiron complex, whose unsubstituted symmetric derivative, **1a**$^+$, belongs to class III, instead of class II. For this mixed valence complex, a delocalized ground state was found, in opposition to simple expectations based on its asymmetry. An explanation based on direct Fe−Fe interaction in the mixed valence cation was invoked.

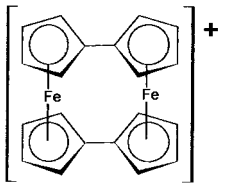

1a$^+$

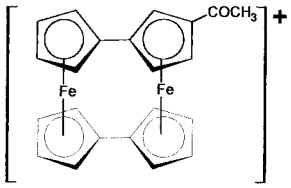

1b$^+$

The aim of this paper is to investigate the effect of the change of the potential energy barrier for electron transfer in the mixed valence complexes [Cp*Fe(pentalenyl)MCp*]$^+$, with M = Fe (**2a**$^+$) and M = Co (**2b**$^+$). Specifically, this was achieved by introducing asymmetry in the complexes by the replacement of one of the pentamethylcyclopentadienyl ligands by an hydropentalenyl group (**3a**$^+$, **3b**$^+$).

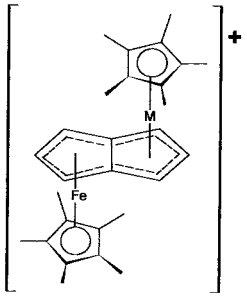

2a$^+$ M = Fe; **2b**$^+$ M = Co

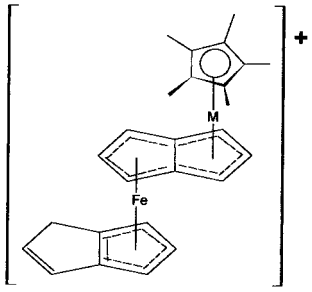

3a$^+$ M = Fe; **3b**$^+$ M = Co

Parent compounds **2a**$^+$ and **2b**$^+$ have been previously reported to have delocalized and localized ground states, respectively.[16] Given that the anti conformation of the two metal atoms in these complexes precludes direct metal-to-metal interaction, as observed for **1a**$^+$ and **1b**$^+$, any electronic coupling eventually observed would originate through bond interactions exclusively, facilitated by the bridging ligand. Specifically, the comparison of **2a**$^+$ and **3a**$^+$ offers the possibility to study the effect of asymmetry in the case where the symmetric derivative belongs to class III. On the other hand, the comparison of **2b**$^+$ and **3b**$^+$ allows the study of the influence of asymmetry on a heterobinuclear mixed valence class II complex. To our knowledge, the influence of both of these factors on the rate of intramolecular electron transfer has not been deeply studied.

Experimental Section

Materials. All reactions were carried out using Schlenk techniques under nitrogen atmosphere, and the products were subsequently handled in a dry oxygen-free glovebox. Solvents used were predried and distilled from appropriate drying agents. The neutral precursors [Cp*Fe(C_8H_6)Fe(C_8H_7)] and [Cp*Co(C_8H_6)Fe(C_8H_7)] were synthesized following the synthetic methods suggested by Manríquez et al.[17] The compounds were isolated and conveniently characterized. The oxidant, $Cp_2FeBAr'_4$, was synthesized as reported in the literature.[18]

Preparation of [Cp*Fe(C_8H_6)Fe(C_8H_7)]BAr'_4, [3a$^+$]BAr'_4. [Cp*Fe(C_8H_6)Fe(C_8H_7)][17] (156 mg, 0.345 mmol) and Cp_2FeBAr_4[18] (362 mg, 0.345 mmol) were dissolved in 15 mL of diethyl ether (Aldrich), and the mixture was stirred at room temperature for 30 min resulting in the formation of a violet solution. Petroleum ether (45 mL) was added, and the precipitate formed was filtered, washed with petroleum ether, and dried under vacuum. The solid was recrystallized by slow diffusion of petroleum ether (Aldrich) into a concentrated diethyl ether solution of [Cp*Fe(C_8H_6)Fe(C_8H_7)]BAr'_4, **[3a**$^+$**]BAr'**$_4$. Violet crystals (83%) were observed within 24 h. The crystals were filtered, washed with petroleum ether, and dried under vacuum. The solid obtained was paramagnetic. IR (Nujol): 1612 (m), 1276 (s, BAr_4^-), 1133 (vs, BAr_4^-), 887 (m), 839 (m), 814 (w), 727 (m), 713 (m), 682 (m), and 669 cm^{-1} (m). Elemental analysis for $C_{58}H_{40}BF_{24}Fe_2$ with a molecule of diethyl ether ($C_4H_{10}O$): Calcd C, 53.59%; H, 3.63%. Found C, 53.75%; H, 3.60%.

Preparation of [Cp*Co(C_8H_6)Fe(C_8H_7)]BAr'_4, [3b$^+$]BAr'_4. A solution of [Cp*Co(C_8H_6)Fe(C_8H_7)][17] (150 mg, 0.330 mmol) in diethyl ether (15 mL) (Aldrich) was added to Cp_2FeBAr_4[18] (346 mg, 0.330 mmol) and the mixture stirred at room temperature for 30 min resulting in the formation of a blue solution. Petroleum ether (45 mL) (Aldrich) was added and the precipitate filtered, washed with petroleum ether, and dried under vacuum. The solid was recrystallized by slow diffusion of petroleum ether into a concentrated diethyl ether solution of **[3a**$^+$**]BAr'**$_4$. Blue crystals (85%) were observed within 24 h. Crystals were filtered, washed with petroleum, and dried under vacuum. ^{1}H NMR (CD_2Cl_2): 1.60 (s, 15H, Cp*), 2.67 (m, 2H), 3.8 (t, 1H), 4.2 (t, 1H), 4.3 (d, 1H), 4.5 (d, 1H), 4.6 (t, 1H), 5.1 (d, 1H), 5.2 (t, 2H), 6.17−6.30 (dd, 2H), 7.57 (s, 4H, BAr_4^-), and 7.73 (s, 8H, BAr_4^-). IR (Nujol): 1612 (w), 1284 (s, BAr_4^-), 1154−1133 (vs, BAr_4^-), 887 (m), 839 (w), 807 (w), 725 (m), 714 (m), 682 (m), 669 cm^{-1} (m). Elemental analysis for $C_{58}H_{40}BF_{24}FeCo$: Calcd C, 52.94%; H, 3.04%. Found C, 52.65%; H, 3.02%.

Instrumentation. IR spectra were recorded on a Perkin-Elmer 1710 FT spectrophotometer using a solution of the complex in Nujol. Elemental analyses were carried out with a Fison 1108 microanalyzer. ^{1}H NMR spectra were recorded on a GE/QE-300

(16) Manriquez, J. M.; Ward, M. D.; Reiff, W. M.; Calabrese, J. C.; Jones, N. L.; Carroll, P. J.; Bunel, E. E.; Miller, J. S. *J. Am. Chem. Soc.* **1995**, *117*, 6182.

(17) Oelckers, B.; Chávez, I.; Manríquez, J. M.; Roman, E. *Organometallics* **1993**, *12*, 3396.

(18) Chávez, I.; Alvarez, A.; Molins, E.; Roig, A.; Maniukiewicz, W.; Arancibia, A.; Arancibia, V.; Brand, H.; Manríquez, J. M. *J. Organomet. Chem.* **2000**, *601* (1), 126.

spectrometer using benzene-d_6. Chemical shifts are reported in ppm relative to an external $SiMe_4$ standard. NIR spectra were performed on a UV−vis−NIR SHIMADZU UV−3101 PC scanning spectrophotometer.

Cyclic voltammetry measurements were carried out with a Bank potentiostat (model Wenking ST-72) coupled to a voltage scan generator (model VSG-72) and a Graphtec recorder (model WX-1100) and with a Bioanalytical Systems voltammetric analyzer (model CV-50w, version 2.3). All operations, viewing, and printing were controlled through the PC using Microsoft Windows. The working electrode was Pt or a glassy carbon disk. The auxiliary electrode was a platinum coil electrode, which was isolated from the bulk solution by a glass tube with a small porosity glass frit at the end. Neutro aluminum oxide was placed on the frit, and the tube was filled with a 0.1 M solution of supporting electrolyte. The reference electrode was a Ag/AgCl wire placed in a tube with a cracked glass bead at the end and containing aqueous tetramethylammonium chloride. The concentration of this solution was varied until the potential value was 0.0 V versus the saturated calomel electrode (SCE).[19] This electrode was located inside a Luggin capillary in the electrochemical cell. The solvents used were ether and dichloromethane. The supporting electrolytes were $NaBAr'_4$ (BAr'_4 = $3,5(CF_3)_2C_6H_3)_4B^-$) for ether and $[N(Bu)_4]BF_4$ (Bu = buthyl) for dichloromethane, respectively. All the experiments were carried out under argon atmosphere, at room temperature (20 °C).

The Mössbauer spectra were obtained using a constant acceleration Mössbauer spectrometer with a $^{57}Co/Rh$ source. The source was moved via triangular velocity waveform, and the γ-counts were collected in a 512 multichannel analyzer. The data were folded, plotted, and fitted by a computer procedure. Velocity calibration was performed using a 25 μm thick metallic Fe foil. The Mössbauer spectral parameters are given relative to this standard at room temperature. The majority of spectra were taken at 70, 80, or 90 K given that the recoil-free factor at room temperature was very low, because of the loose bond of the iron with the ligands.

EPR spectra were obtained on a Bruker EPR 200 spectrometer. Line positions were determined by a Bruker NMR gaussmeter while the microwave frequency was measured by a frequency counter.

Results and Discussion

Synthesis. The mixed valence cations $[Cp^*Fe(C_8H_6)Fe(C_8H_7)]^+$, **3a**$^+$, and $[Cp^*Co(C_8H_6)Fe(C_8H_7)]^+$, **3b**$^+$, were precipitated at first using BF_4^- as counterion. However, the compounds showed kinetic instability, low solubility, and difficulty to crystallize. Other inert anions such as triflate were also unsuccessful. The report in the literature of the new counterion BAr'^-_4 (BAr'^-_4 = $3,5(CF_3)_2C_6H_3)_4B^-$)[20] opened the possibility to synthesize $Cp_2FeBArBAr'_4$ and $Cp^*_2FeBAr'_4$ and use them as selective oxidants.[18] The oxidation of 1 mol of $[Cp^*Co(C_8H_6)Fe(C_8H_7)]$ or $[Cp^*Fe(C_8H_6)Fe(C_8H_7)]$ with 1 mol of $Cp^*_2FeBAr'_4$ afforded the diamagnetic oxidized derivative $[Cp^*Co(C_8H_6)Fe(C_8H_7)]BAr'_4$, **[3b**$^+$**]BAr'$_4$**, as blue crystals, and the paramagnetic compound $[Cp^*Fe(C_8H_6)Fe(C_8H_7)]BAr'_4$, **[3b**$^+$**]BAr'$_4$**, as violet crystals, respectively.

In contrast to the derivatives with BF_4^-, **3a**$^+$ and **3b**$^+$ showed reasonable kinetic and thermodynamic stability in the solid state under dinitrogen, and good solubility. This allowed their characterization and the study of the degree of electronic delocalization in them.

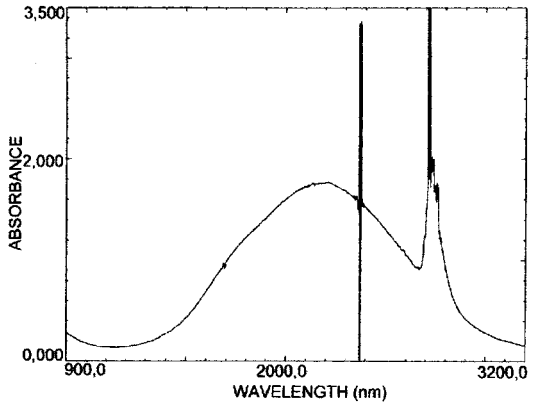

Figure 1. Near-infrared spectra for mixed valence complex $[Cp^*Fe(C_8H_6)Fe(C_8H_7)]BAr'_4$, **[3a**$^+$**]BAr'$_4$**, in CH_2Cl_2 at room temperature.

Table 1. Near-Infrared Band Maxima for $[Cp^*Fe(C_8H_6)Fe(C_8H_7)]BAr'_4$ as a function of solvent

	λ_{max} (nm)	D^a	n^b
acetone	2145	21.00	1.85
THF	2162	7.00	1.98
diethyl ether	2175	4.34	1.84
$CHCl_3$	2191	4.81	2.10
CH_2Cl_2	2169	9.08	2.03

[a] Static dielectric constant. Ref 16. [b] Refraction index. Ref 17.

Electronic Spectroscopy (NIR). Both neutral complexes $[Cp^*Fe(C_8H_6)Fe(C_8H_7)]$ and $[Cp^*Co(C_8H_6)Fe(C_8H_7)]$ have no absorption in the NIR.

The mixed valence **3a**$^+$ cation shows a very broad band at 2187 nm (ϵ = 273.4 M^{-1} cm^{-1}) in CH_2Cl_2, Figure 1, that can be assigned to an intervalence transfer band. For the mixed valence **3b**$^+$ cation, no such band is observed, suggesting the presence of independent metal centers.

The position of the NIR band in **3a**$^+$ is nearly solvent independent; results are shown in Table 1. This result is consistent with strong coupling between the metal centers according to Hush theory.[1b] Moreover, the band maximum of **3a**$^+$ is slightly shifted to the blue in regard to its symmetric analogue, **2a**$^+$, also in agreement with Hush's theory.

Cyclic Voltammetry. The cyclic voltammogram (CV) in ether of complex $[Cp^*Fe(C_8H_6)Fe(C_8H_7)]$, **3a**, at different scan rates showed three quasi reversible processes. The corresponding peak potentials showed dependence on the scan rate. The first redox process was assigned to the $Fe^{II}-Fe^{II} \rightarrow Fe^{II}-Fe^{III}$ oxidation. The corresponding MV species **3a**$^+$ shows the absence of this peak. To understand the origin of the two remaining redox processes, the electrochemical information of bis(η^5-hydropentalenyl)iron, (i.e., the monomeric equivalent of the Fe part of complex **3a**) was considered. For this last compound, a chemical reaction coupled to the one electron electrochemical process was observed.[21] The chemical process was explained considering the high reactivity of the double bond of the hydropentalenyl group. For the bimetallic complex **3a** reported in the present work, we cannot unambiguously ensure which of the two other

(19) Sawyer, D.; Roberts, J. R. *Experimental Electrochemistry for Chemist*; John Wiley and Sons: New York, 1974.
(20) Hauptman, E.; Brookhart, M.; Fagan, P.; Calabrese, J. C. *Organometallics* **1994**, *13*, 774.

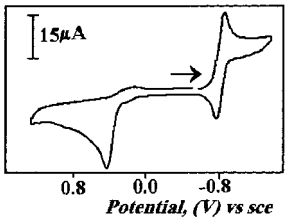

Figure 2. Cyclic voltammogram for complex $[Cp^*Co(C_8H_6)Fe(C_8H_7)]BAr'_4$, **[3b$^+$]BAr′$_4$**, in CH_2Cl_2 (0.1 M in $[N(Bu)_4]BF_4$).

redox events is associated to the $Fe^{II}-Fe^{III} \rightarrow Fe^{III}-Fe^{III}$ process, and which to the oxidation of the hydropentalenyl double bond. It must also be mentioned that the $Fe^{III}-Fe^{III}$ species is very unstable. It was not possible to chemically synthesize it.

The complex $[Cp^*Co(C_8H_6)Fe(C_8H_7)]BAr'_4$, **[3b$^+$]BAr′$_4$**, shows two oxidation waves, the first one corresponding to the Co (II/III) couple and the second to the Fe (II/III) couple. The waves are extremely separated (≈1.4 V) and occur at approximately the same potentials as "ferrocene" and "cobaltocene" type complexes, respectively, Figure 2. This result suggests the presence of two metal centers without interaction.

Mössbauer Spectroscopy. The ^{57}Fe Mössbauer spectra of the neutral compounds and the mixed valence compounds were done. Table 2 gathers the Mössbauer hyperfine parameters for $[Cp^*Fe(C_8H_6)Fe(C_8H_7)]$, **3a**, and $[Cp^*Co(C_8H_6)Fe(C_8H_7)]$, **3b**, (neutral compounds) and $([Cp^*Fe(C_8H_6)Fe(C_8H_7)]BAr'_4$, **[3a$^+$]BAr′$_4$** and $[Cp^*Co(C_8H_6)Fe(C_8H_7)BAr'_4$, **[3b$^+$]BAr′$_4$**, (mixed − valence compounds). Figure 3 shows the Mössbauer spectra of the four complexes.

Complex **3a** was measured at low temperature and was fitted to a single doublet (see Figure 3a). The spectrum exhibits a large "ferrocene-like" quadrupole splitting, $\Delta E_q = 2.37$ mm/s (at 90 K), characteristic of Fe^{2+}. The Mössbauer spectrum of the neutral iron−cobalt system, **3b**, also corresponds to a "ferrocene-like" system with the electron spin residing on the low-spin Co^{II} (see Figure 3b). The spectrum was also fitted to a single doublet associated to Fe^{2+}.

The spectrum of mixed valence compound **[3a$^+$]BAr′$_4$** was fitted using four symmetrical doublets (see Figure 3c). The main contribution to the total area (71%) has been assigned to the iron sites with an intermediate valence ($Fe^{+2.5}$). The value of the quadrupolar splitting for these sites is 1.3 mm/s; this value is in consonance with that found in a previous report,[16] meaning that the velocity of electron transfer between the two metallic centers is faster than the Mössbauer time scale (10^{-7} s^{-1}) and thus revealing a delocalized behavior, corresponding to electron coupling between metal sites.

The other three sites have been assigned to Fe^{2+}, Fe^{3+}, and Fe^{2+}, respectively. The Fe^{2+} site with a 10% fraction of the total area has similar Mössbauer spectral parameters of the initial compound; therefore, a small fraction of the neutral compound did not react with the oxidant. The site assigned to Fe^{3+} (5% of the total area) could be due to a side product from the double oxidation of a very small fraction of the sample. The remaining residual 14%, in view of the spectral values, should be assigned to Fe^{2+}. The higher isomer shift value observed in this case suggests an ionic bonding character of the iron atom and does not correspond to the typical ferrocene-like iron species. Considering the high sensibility of the compound to air, the most feasible explanation is that this compound originates from a minor sample alteration. Nevertheless, the possibility of a side chemical path leading to an unknown compound should not be excluded. It should be emphasized at this point that, despite the minor contributions of side products, the main contribution to the Mössbauer spectra is clearly an $Fe^{2.5}-Fe^{2.5}$ species, assigned to the $[Cp^*Fe(C_8H_6)Fe(C_8H_7)]^+$, **3a$^+$**, cation, that therefore behaves as a fully delocalized MV compound in the Mössbauer time scale.

The iron−cobalt salt has been fitted to a single symmetrical doublet (see Figure 3d). Interestingly, the Mössbauer spectrum of the monocation is also like that of ferrocene, indicating the selective oxidation of the cobalt. This result is also confirmed by NMR because the neutral compound **3b** is paramagnetic while the mixed valence compound **[3b$^+$]BAr′$_4$** is diamagnetic, indicating the stability of the low-spin d^6 configuration.

Electron Paramagnetic Resonance. The EPR spectra of the mixed valence **[3a$^+$]BAr′$_4$** complex, at 293 and 100 K, were recorded, Figure 4. The spectrum at 100 K reflects a significantly low *g*-factor anisotropy with $\Delta g = |g_{\parallel} - g_{\perp}| = 0.45$.[16] Species exhibiting *detrapping* on the EPR time scale, corresponding to rates of intramolecular electron-transfer greater than 10^9-10^{10} s^{-1}, have different electronic states with much lower *g* anisotropy than analogous *trapped* species.[22] For example, [Cp*Fe(pentalene)FeCp*]BF_4, **[2a$^+$]BF$_4$**, which is shown to be completely delocalized, has a *g* anisotropy of 0.45; however, [Cp*Fe(as-indacene)FeCp*]BF_4, a trapped compound, has $\Delta g = 1.52$ (solid state).[16] Other cases reported in the literature also show the same trend. Thus, $[(fulvalene)_2Fe_2]^+I_5^-$, which was shown to be completely delocalized by IR spectroscopy, has a *g* anisotropy corresponding to $\Delta g = 0.41$ in the solid state.[22,23] However, $([(fulvalene)\{Fe(C_5H_4Cl)\}_2]^+)_2I_8^{2-}$, trapped on the Mössbauer time scale, has $\Delta g = 1.40$ in the solid state.[22,24] According to the previously described analysis, the **[3a$^+$]BAr′$_4$** complex reported in this work shows a behavior corresponding to valence detrapping. This is consistent with the results of Mössbauer spectroscopy described in the previous paragraph.

The **[3b$^+$]BAr′$_4$** complex was EPR silent, as expected for the combination of diamagnetic low-spin Fe(II) and diamagnetic low-spin Co(III).

Conclusions

The spectroscopic results (NIR, Mössbauer, EPR, etc.) for the $[Cp^*Fe(C_8H_6)Fe(C_8H_7)]BAr'_4$ complex reveal delocal-

(21) Oelckers, B., MSc. Thesis, Universidad Técnica Federico Santa María, 1994.

(22) Barlow, S.; O'Hare, D. *Chem. Rev.* **1997**, *97*, 637−669.
(23) Morrison, W. H.; Hendrickson, D. N. *Inorg. Chem.* **1975**, *14*, 2331.
(24) Dong, T.-Y.; Hendrickson, D. N.; Pierpont, C. G.; Moore, M. F. *J. Am. Chem. Soc.* **1986**, *108*, 963.

Table 2. Hyperfine Parameters from the Fitting of the Mössbauer Spectra[a]

	T (K)	site	δ_{Fc} (mm s^{-1})	ΔE_q (mms^{-1})	Γ (mm s^{-1})	area (%)	χ^2
			Neutral Compounds				
[Cp*Fe(C_8H_6)Fe(C_8H_7)]	90	Fe^{2+}	0.552(1)	2.37(1)	0.25(1)	100	1.4
[Cp*Co(C_8H_6)Fe(C_8H_7)]	80	Fe^{2+}	0.559(1)	2.10(1)	0.28(1)	100	1.2
	300	Fe^{2+}	0.481(1)	2.10(1)	0.26(1)	100	1.2
			Mixed Valence Compounds				
[Cp*Fe(C_8H_6)Fe(C_8H_7)]BAr'_4	70	Fe^{2+}	0.50(1)	2.54(1)	0.27(3)	10	1.0
		$Fe^{2.5+}$	0.53(8)	1.3(2)	0.45(2)	71	
		Fe^{3+}	0.52(3)	0.41(5)	0.33(8)	5	
		Fe^{2+}	1.2(4)	2.6(7)	0.42(2)	14	
[Cp*Co(C_8H_6)Fe(C_8H_7)BAr'_4]	90	Fe^{2+}	0.562(1)	2.25(1)	0.22(1)	100	1.2

[a] δ_{Fe}, ΔE_q, and Γ are the isomer shift, the quadrupole splitting, and the full width at half maximum, respectively. The area represents the Mössbauer fraction of each subspectrum in relative percentage of each subspectrum. The errors are given within brackets and correspond to the last digit.

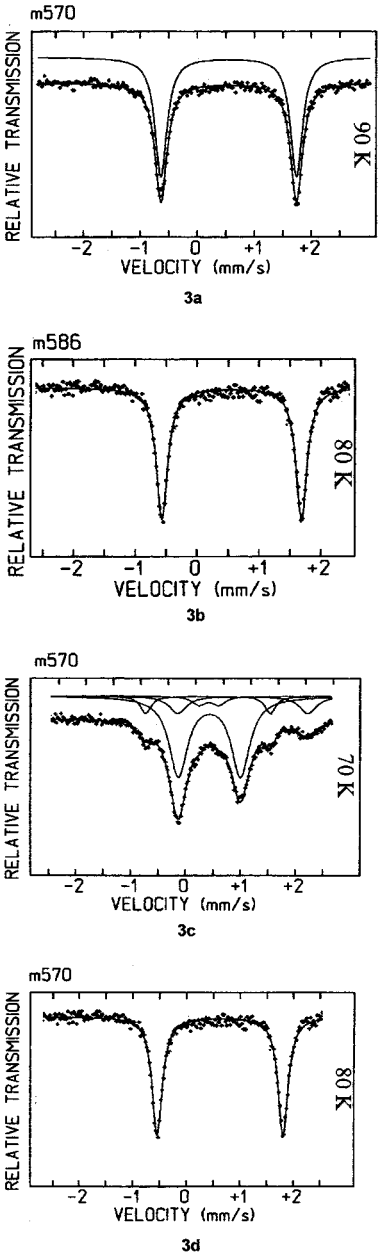

Figure 3. Mössbauer spectra of [Cp*Fe(C_8H_6)Fe(C_8H_7)]^n and [Cp*Co(C_8H_6)Fe(C_8H_7)]^n (n = 0, 1+): (a) [Cp*Fe(C_8H_6)Fe(C_8H_7)], (b) [Cp*Co(C_8H_6)Fe(C_8H_7)],(c)[Cp*Fe(C_8H_6)Fe(C_8H_7)]BAr_4^-,(d)[Cp*Co(C_8H_6)Fe(C_8H_7)]BAr_4^-.

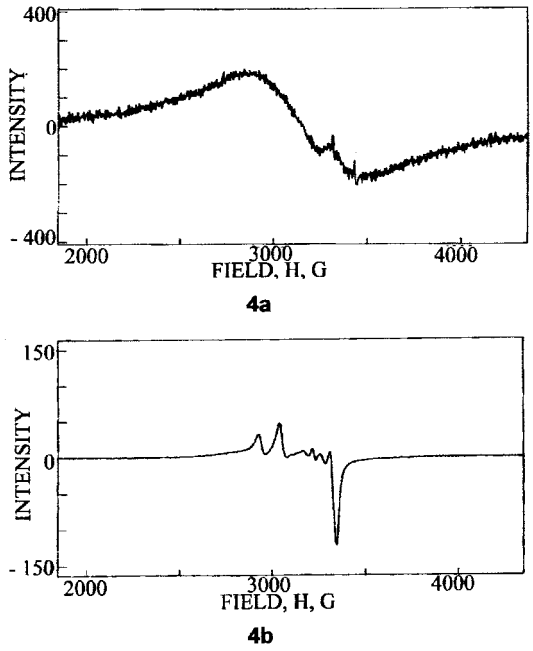

Figure 4. EPR spectra of [Cp*Fe(C_8H_6)Fe(C_8H_7)]BAr'_4 in CH_2Cl_2 at 293 K (a) and 100 K (b).

ized behavior, corresponding to electron coupling between metal sites. The mixed valence complex exhibits an intervalence charge transfer absorption band. This intervalence transfer band is nearly solvent independent, reflecting electronic delocalization. The value of the quadrupolar splitting for Mössbauer spectra is 1.3 mm/s, meaning that the velocity of electron transfer between the two metal centers is faster than the Mössbauer time scale (10^{-7} s^{-1}). EPR spectra reflect a factor anisotropy with $\Delta g = |g_{\parallel} - g_{\perp}| = 0.45$, corresponding to valence detrapping. Following Robin and Day's classification, the compound should be assigned to class III. This experimental behavior reveals that, despite the barrier introduced by the asymmetry of the complex, compound **[3a$^+$]BAr'$_4$** retains the delocalized behavior of its symmetric analogue, **2a**$^+$. Similar behavior was observed by Moore and Hendrickson[14] for the compounds **1a**$^+$ and **1b**$^+$ shown in the Introduction. In their case, Fe−Fe interaction was invoked to explain this phenomenon. The anti conformation of the **3a**$^+$ cation demonstrates that the bridging ligand must play an important role in permitting an intense communication between the metal centers. On the other hand, the experimental behavior described also demonstrates that the barrier introduced, in this case by an asymmetry in the terminal ligands, must be low.

The $[Cp^*Co(C_8H_6)Fe(C_8H_7)]BAr'_4$ complex has no intervalence transfer band. This is puzzling, considering that its symmetric analogue $\mathbf{2b}^+$ has an IT band at 1038 nm.[16] The asymmetry of the compound could have shifted the band to higher energy, being obscured by the other bands of the complex. The cyclic voltammogram in this case exhibited two waves at approximately the same potential as the "ferrocene" and "cobaltocene" type complexes, respectively. Mössbauer spectra were typical spectra of Fe(II), implying a selective oxidation of the Co metal center. This compound is a clear example of a Class I complex following Robin and Day's classification.

Analyzing the experimental results in a comparative way, the different behavior observed for $[Cp^*Fe(C_8H_6)Fe(C_8H_7)]BAr'_4$, $\mathbf{[3b^+]BAr'_4}$, and $[Cp^*Co(C_8H_6)Fe(C_8H_7)]BAr'_4$, $\mathbf{[3b^+]BAr'_4}$, is understandable, considering their homonuclear and heteronuclear natures, respectively. The different electronic nature of Co in regard to Fe produces a dramatic change in the barrier for electron transfer, reflected in a change in behavior from delocalized in $\mathbf{[3b^+]BAr'_4}$ to localized in $\mathbf{[3b^+]BAr'_4}$. Interestingly, the effect of changing a terminal ligand on the barrier is different for delocalized compounds than for localized ones. Specifically, only subtle changes are observed when comparing the behavior of the delocalized $\mathbf{2a}^+$ and $\mathbf{3a}^+$ compounds. A more dramatic effect is observed by comparing localized compounds $\mathbf{2b}^+$ and $\mathbf{3b}^+$, where the first has an IT band that is not observed in the second.

Acknowledgment. We gratefully acknowledge financial support of this work by FONDECYT 2990103 and FONDECYT Líneas Complementarias 8980007. The exchange Project 2001CL0027 between CSIC and CONICYT is also acknowledged. We want to thank to Dr. Ana María Leiva and the technical assistance provided by Dr. Pierre Rivière and Dr. Monique Rivière.

IC011175S